

FATIGUE DAMAGE OF 2024-T351 ALUMINIUM ALLOY FRICTION STIR WELDING JOINTS. PART 2: FATIGUE DAMAGE

Aidy Ali^{1*}, Mike W. Brown² and Omar Suliman Zaroog¹

Received: Jul 8, 2008; Revised: Sept 15, 2008; Accepted: Sept 18, 2008

Abstract

The characterisation of micro and macro mechanics in 2024-T351 (Al Alloy) FSW joints was conducted to identify the critical regimes for natural fatigue crack initiation in 2024-T351 Al Alloy FSW welded joints and was presented in Part 1. In this Part, the fatigue tests were performed. Scanning electron microscopy analysis on fracture surfaces revealed that natural crack initiates from multiple sites and is propagated through different regimes causing coalescence. Replicas of crack images confirmed that multiple cracks coalesce. The natural fatigue initiation sites which were found begin from subsurface defects rather than form a free surface. For a different applied stress level, the initiation sites were changed from one regime to another. The number of cracks observed reduces as the applied stress drops. The fatigue limit of this welded joint was governed by a coalescence of the cracks rather than by the propagation.

Keywords: 2024-T351 Aluminium alloy, crack coalescence, fatigue, friction stir welding

Introduction

Commercial transport airplanes generally consist of a built-up structure where the skin-to-stringer connection may be riveted or bonded. The other connections such as skin-clip (shear ties) and clip-frames are riveted. The material used in general is the aluminium 2000 series (2024, 2524) for all elements. In specific areas the 7000 series alloys (7475, 7075, 7349) are used to increase the strength (Kissell and Malloy, 2001; Schmidt *et al.*, 2001). The design of future aircraft struc-

tures has to consider forthcoming joining techniques and the regulations. For many years, damage tolerant design has been used extensively in aircraft structure and consists of a lot of riveted joints and the primary goals for this design are to guarantee the structural safety and the optimum performance of the aircraft structure. Today, the goal is the same but, driven by cost and weight savings, technology progress is moving in the direction of replacing rivets

¹ *Fatigue and Fracture Research Group, Department of Mechanical and Manufacturing Engineering, University of Putra Malaysia, 43400 Serdang, Selangor, Malaysia. E-mail: aidy@eng.upm.edu.my*

² *Department of Mechanical Engineering, The University of Sheffield, Mappin Street, Sheffield, S1 1JD, United Kingdom.*

* *Corresponding author*

with welds. Consequently, if the welded structure can match the riveted joints in terms of structural integrity there are issues in a damage tolerance design that need to be resolved. For instance, the use of welds instead of riveted joints will have a profound impact on the fatigue crack initiation, propagation and safety in aircraft. Placing a weld into a structure will:

- a) Cause a local modification of the crack initiation site and the propagation direction.
- b) Cause local modification of the micro-structure in the fusion zone. Solid-state processes such as friction stir welds will have a drastically modified grain structure.
- c) Result in the heating cycle softening the parent alloy in the zones on either side of the weld line. In friction stir welds it has been reported that 2024-T351 alloy reduces in hardness from 140 Hv1 in the parent plate to just over 100 Hv1, (Jata and Semiatin, 2000), a reduction of almost 30%.
- d) Result in the weld thermal cycle introducing substantial residual stress fields which remain after the process is complete. The major stress is tensile parallel with the weld axis, decreases with increased distance from the weld and is balanced by a compressive stress at further distance from the weld.
- e) Result in the weld surface relief causing a stress concentration, which will reduce fatigue performance on un-machined welds. For this reason it is likely that welds on aircraft will be used in the surface skimmed condition to remove these sources of fatigue strength degradation (Bussu and Irving, 2001).
- f) Result in welding processes producing defects or impurities. These defects could be like vacancies, interstices and surface cracks.
- g) Result in a huge weight saving from elimination of the weight of many steel bolts and rivets.
- h) By virtue of the absence of a contact surface in the joint of the structure or plate, automatically eliminate the fretting fatigue problems as in riveted lap joints.
- i) Enable the structure to be constructed for a dissimilar alloy as for a riveted joint one.

From the above impact list, the challenge

of replacing riveted aircraft structures by welding is no longer about the difficulty of welding high strength alloys, but the issue is how a damage tolerant design approach for welded aircraft structures can be applied. In the near future, BAE System planes (A318 and A3XX) will feature fuselage stringers laser-welded to the airplane skin. Looking further into the future, it is likely that friction stir welding will be applied on airplane structural components. since it can reliably join alloy of the series 2000 and 7000. Friction stir welding is also likely to play a significant role by enabling the fabrication of blisks for military engines (Mendez and Eagar, 2001).

Friction stir welding (FSW) is a solid state welding process that has received worldwide attention, particularly for joining aluminium alloys (Kissell and Malloy, 2001; Schmidt *et al.*, 2001). An FSW joint seems to be a high potential technique for joining high strength Al Alloy, and is most promising as an alternative way to replace bolt joints then giving weight reduction. On the other hand, a damage tolerant design is still the best design approach to maintain the cost and weight saving for aircraft structure manufacturing. The damage tolerant approach demands a knowledge of fatigue crack detection, initial crack length, propagation direction, fatigue crack growth rate, and maximum tolerable crack length to determine an appropriate inspection time interval. The extensive use of FSW airframe components therefore represents an important shift in the treatment of damage tolerance in airframes, requiring a better understanding of crack initiation characteristics and corresponding implications for crack growth.

In this paper we present the fatigue data for FSW of 2024-T351 Al Alloy. Scanning electron microscopy (SEM) analysis (Jata and Semiatin, 2000) on fracture surfaces, energy dispersive X-ray analysis (EDX), and replication techniques were used to pinpoint the initiation site and fatigue failure mechanism. The results of this research will assist the designer to predict the fatigue life of friction stir welded aircraft structure. Ultimately the manufacturer can make a sound basic decision whether or not

to use this joint for aircraft applications.

Experimental Procedure

The investigation was performed on 13 mm thick plate of 2024-T351 Al Alloy. The FSW was provided by Airbus UK Ltd. Plates $75 \times 60 \times 13$ mm were welded along their long edge with the weld direction parallel to the longitudinal (rolling) orientation. The Demec dial gauge was used to measure the strain on the top and bottom of the weld plate in order to avoid any possible residual stress relief due to specimens being sliced from the initial plate, so that the specimens made truly represented the proper-

ties of the real FSW weld joints as shown in Figure 1.

Fatigue endurance tests were carried out on a longitudinal specimen with a length of 80 mm and width of 60 mm in a four-point bending test in accordance with ASTM D6272 (ASTM 1998) at a constant load amplitude, constant frequency of 20 Hz, and a stress ratio R of 0.1. The specimen and bending test configuration are shown in Figure 2 which provides the uniform stress area encompassing the main features of the weld regions. In order to see the effect of surface roughness and defects, the welded specimens surfaces were mechanically polished to a $1/4$ micron finish. Fracture surfaces

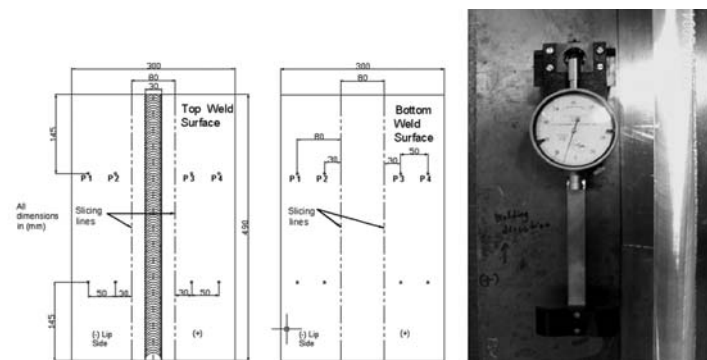


Figure 1. Measured strain location with Demec dial gauge

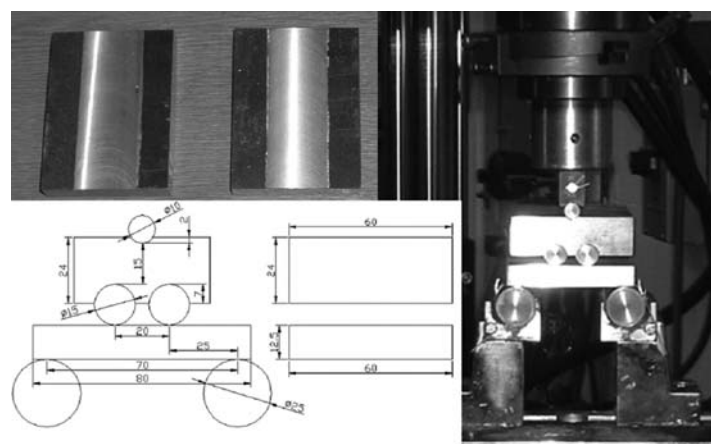


Figure 2. The specimen image and bending test configuration

were examined optically, in the SEM (Jata and Semiatin, 2000) and EDX analyses. The method used for crack detection was made by employing the acetate replication technique combined with optical microscopy to provide a digital crack images. Crack measurements were taken from replication images using the Sigma Scan analysis software.

Results and Discussions

Stress reliefs measured from the Demec dial gauge after slicing were 0.263 MPa and 0.2418 MPa for the top and bottom welded plate

surfaces respectively, which are considered small and negligible. Having quantified the amount of residual stress relief from slicing the specimens, we confirmed that the chosen specimen dimension was not distorted by the initial residual stress induced from the weld processing.

Figure 3 represents the stress vs. number of cycle to failure (S-N) data for the parent material and FSW as-welded specimens. Obviously there is a tremendous drop in the fatigue strength of FSW as-welded compared with the parent plate. Since surface irregularities can degrade the fatigue strength, Figure 4 shows the S-N data for FSW as-welded and FSW

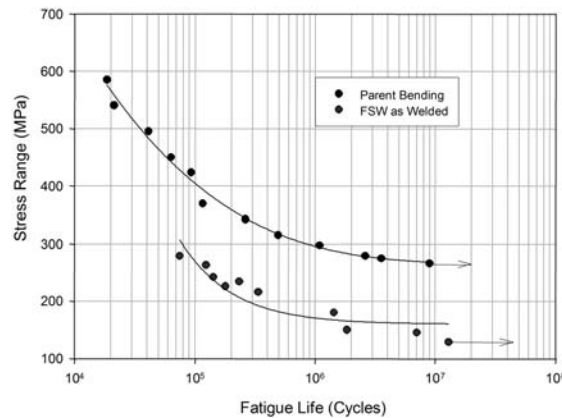


Figure 3. Stress life curves for FSW as welded versus parent plate of 2024-351 AL Alloy with load ratio $R = 0.1$

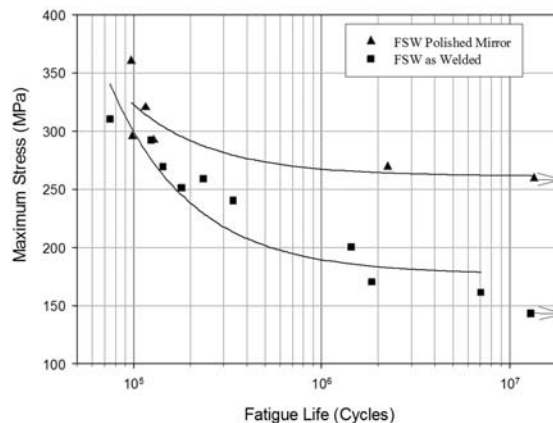


Figure 4. Stress life curves for FSW as welded versus FSW polished mirror of 2024-T351 AL Alloy with load ratio $R = 0.1$

mirror-polished specimen. It is worth noting that there is a significant life improvement was found, specifically in the high cycle fatigue (HCF) regime when the surface irregularities were removed by the mechanical polishing. Fatigue is hailed as a defect sensitive property. As a rule of thumb, any parameter that will increase the local stress concentration will also degrade fatigue performance. How surface irregularities can degrade fatigue strength, especially in the HCF regime is investigated using SEM and EDX analysis. In order to investigate the initiation origin and its causes, two fracture surfaces were taken from the HCF and low cycle fatigue (LCF) regimes in both FSW as-welded and FSW polished mirror and were examined.

After careful SEM investigation, it was found the exact natural crack initiation origin in FSW 2024-T351 was influenced by the stress level and the severity of surface irregularities. The multiple cracking was confirmed causing the crack coalescence and degrading in fatigue performance.

In this sample, (LCF of 2024-T351 AL Alloy FSW as welded) the initiation location was observed nucleating from -1 mm from the plate joint line (PJL) (in the Flow arm) and two cracks initiated at -15 mm and 17 mm from the PJL (in the heat affected zone (HAZ)). As the stress amplitude decreases, the number of cracks seems to be reduced into two cracks rather than three

observed in the low stress/HCF regime. In this case, crack initiation was found at -13 mm from the PJL, where it falls at the end of thermo-mechanically affected zone (TMAZ) regime, and at which the lip exists. It seems as if the lip introduced a stress concentrator which caused the fatigue crack to initiate. The second crack was found at 1mm from the PJL (in the Flow Arm), which was predominantly from the free surface roughness of the welding beach mark.

However, when the surface roughness irregularities were removed by means of polishing, the initiation site was changed; from the HAZ to -5 mm and -6 mm from the PJL, which are located at the end of the Flow arm regime, the beginning of the TMAZ, and underneath at the end of the nugget regime which can be named as the triple point position as shown in Figure 5. Multiple cracking also has been observed in the polished specimen in the LCF regime. When the stress reduces, the crack coalescence is not observed, and only the single crack initiation was found in the HCF of the polished specimen which mainly initiated at -6 mm from the PJL where the transition of the Flow Arm to the TMAZ begins. It is worth noting that each micro-regime in FSW seems to have a different fatigue threshold individually; when high stress is applied, it overcomes the entire threshold causing a multiple cracking phenomenon. On the other hand, once the stress reduces, the multiple cracking is gone;

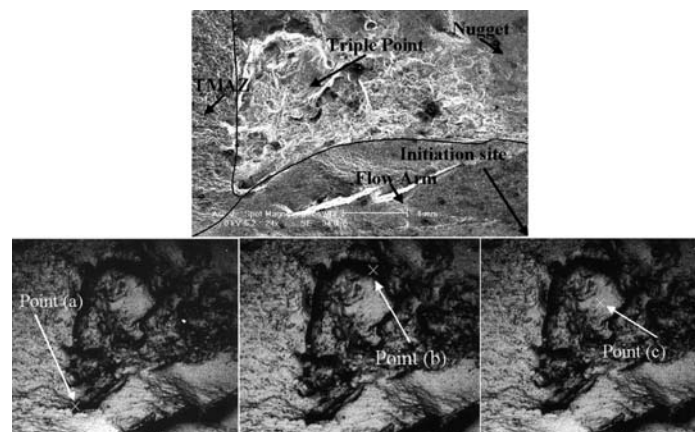


Figure 5. SEM fractograph and EDX analysis position of initiation images for LCF of 2024-T351 AL Alloy FSW as welded specimen at 292 MPa applied stress with load ratio $R = 0.1$

it causes the crack to be initiated at the lowest micro-regime threshold value, which is believed to cause the single cracking phenomenon.

Further investigation was carried out to take advantage of the higher resolution in SEM and, working together with the EDX analysis, revealed the initiation site in FSW. Figure 5 illustrates the initiation site in the LCF FSW as-welded. It is evident that the crack was initiated from the free surface, propagating to the triple point regime, and causing a severely fractured surface. We used the EDX analysis to investigate any inclusion in the triple point location at several positions which were labelled as Point (a), Point (b) and Point (c) as shown in Figure 5. Table 1 represents the chemical composition of the material at each position of interest from the EDX analysis. Point (b) exhibits an enormous amount of oxygen (54.43%) which is believed to cause formation of the severely fractured surface that accelerates the crack growth and which is located approximately 3 mm from the top free surface of the weld. Nevertheless, both position Point (a) and (c) exhibit small amount of oxygen confirmed by the mechanism in the triple point regime where the grain is severely elongated due to stirring in the FSW process.

In the LCF of the polished sample, the initiation site started at the transition zone

between the Flow Arm and Nugget regime with approximately 50 - 100 μ m depths as shown in Figure 6. EDX analysis which was performed at three positions of interest shown in Figure 6. The figure revealed that, one of the cracks started from broken or debonded precipitate at Point (c) and oxygen was also found in this transition zone as shown in Figure 7. It is worth noting that one of the initiations was mainly started at a silicon oxide inclusion at Point (a) which contains 66.42% of silicon and 11.25% oxygen as summarised in Table 2; that caused the subsurface crack initiation to occur. Further EDX analysis passing the transition zone at Point (b) revealed there is no clear indication of an inclusion and a high amount of trapped oxygen.

For the HCF of the polished sample, when the crack surface was observed at high magnification, the crack initiation point was shown to have initiated inside the Flow arm causing severe damage experienced by the material at the triple point regime as illustrated in Figure 8. In order to reinforce the idea that the inclusion was part of the material prior to failure, EDX spots at Point (a) in Figure 8 were selected at the perimeter of the inclusion. As a result, a white feature in Figure 8 was analysed and found to contain an inclusion with 67.07% silicon and 12.13% oxygen in the composition as summarised in Table 3. Further high magnification near

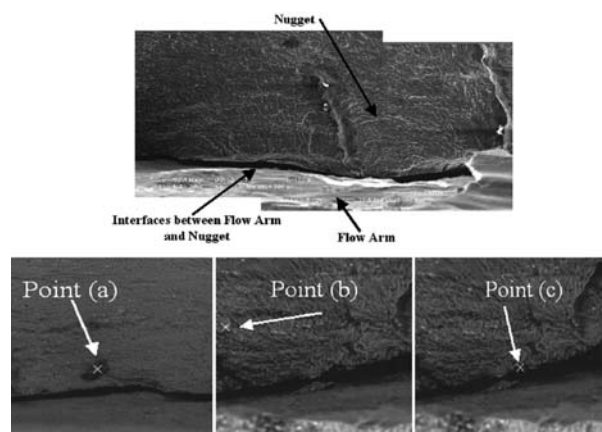


Figure 6. SEM fractograph and EDX analysis position of initiation images for LCF of 2024-T351 AL Alloy FSW polished mirror specimen at 300 MPa applied stress with load ratio $R = 0.1$

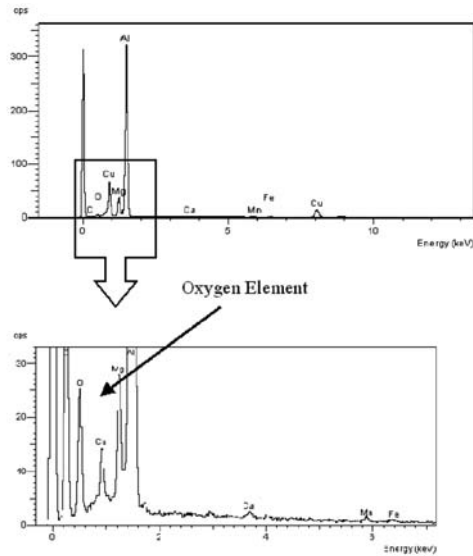


Figure 7. EDX analysis showed that the chemical composition of the material at position point (c) LCF of 2024-T351 ALAlloy FSW polished mirror specimen at 300 MPa applied stress with load ratio R = 0.1

Table 1. Chemical composition of the material at certain positions analysed from EDX for LCF of 2024-T351 ALAlloy FSW as-welded specimen at 292 MPa applied stress with load ratio R = 0.1

Elements	Point (a) (%)	Point (b) (%)	Point (c) (%)
O	8.63	54.43	2.78
Al	85.75	41.70	91.49
Mn	0.65	0.46	0.64
Fe	0.26	0.07	0.24
Cu	4.71	3.34	4.85

Table 2. Chemical composition of the material at certain positions analysed from EDX for LCF of 2024-T351 ALAlloy FSW mirror-polished at 300MPa applied stress with load ratio R = 0.1

Elements	Point (a) (%)	Point (b) (%)	Point (c) (%)
O	11.25	2.19	5.82
Al	16.16	92.99	91.11
Mn	0.34	-	1.01
Fe	1.24	0.10	-
Cu	2.57	4.13	2.06
Si	66.42	-	-
Ti	1.67	-	-
Ni	0.35	-	-

the surface, by SEM analysis, confirmed the existence of trapped gaseous elements within the Flow Arm as shown in Figure 9.

Having analysed the SEM and EDX results, the fatigue initiation of FSW 2024-T351 AL Alloy was influenced by material defects such as inclusion and porosity. Replica images for the mirror-polished LCF specimens in Figure 10 confirm the occurrence of multiple crack initiation, causing crack coalescence and overlapping. On the other hand, the replicas images captured from the HCF of the polished samples shown in Figure 11 confirm a single crack initiation and propagation until final fracture.

When defects are likely to be present, the initiation phase is very short and major fatigue life will be spent in crack propagation. An additional parameter can be tensile residual stresses present in the triple point location, which increases the loading range and may accelerate fatigue crack propagation.

Conclusions

1. SEM, EDX, and surface replica tech-

niques were successful to point out the fatigue initiation site and its location in FSW 2024-T351 AL Alloy joints.

2. Crack coalescence occurring in the high stress/LCF regime was due to high stress that was successful to overcome the fatigue resistance of multiple micro-regime in FSW joints.

3. The single crack observed in the low stress/HCF regime was due to the crack initiated

Table 3. Chemical composition of the material at certain position analysed from EDX for HCF of 2024-T351 AL Alloy FSW polished mirror at 270 MPa applied stress with load ratio $R = 0.1$

Elements	Point (a)
O	12.13
AL	16.25
Mn	0.34
Fe	1.25
Cu	2.60
Si	67.07
Ni	0.35

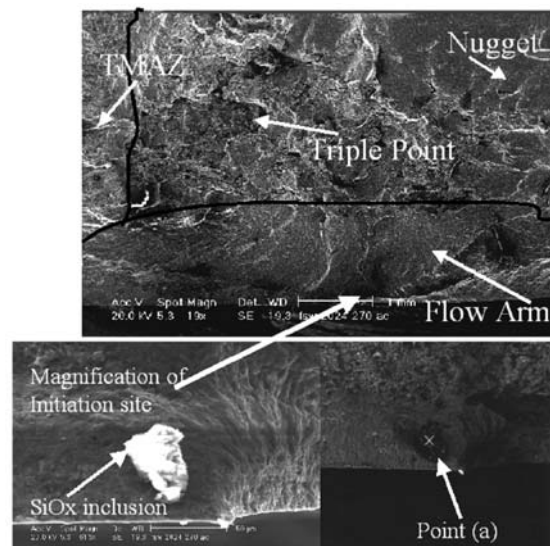


Figure 8. SEM fractograph and EDX analysis position of initiation images for HCF of 2024-T351 AL Alloy FSW polished mirror specimen at 270 MPa applied stress with load ratio $R = 0.1$

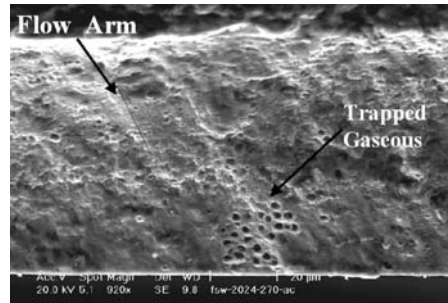


Figure 9. SEM fractograph confirm the existence of trapped gaseous elements at near surface depth within the flow arm for HCF of 2024-T351 AL Alloy FSW polished mirror specimen at 270 MPa applied stress with load ratio $R = 0.1$

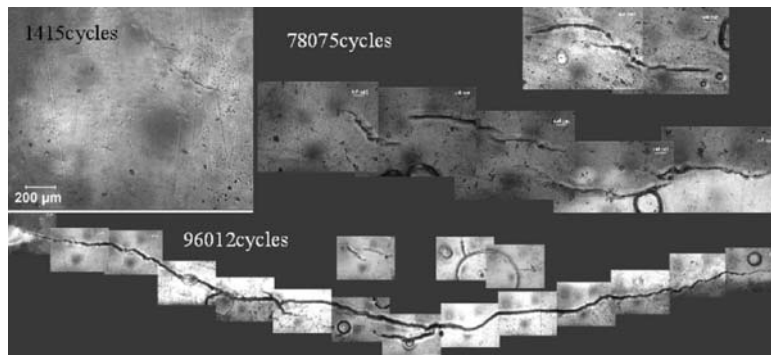


Figure 10. Replica images for LCF of 2024-T351 AL Alloy FSW polished mirror specimen at 300 MPa applied stress with load ratio $R = 0.1$

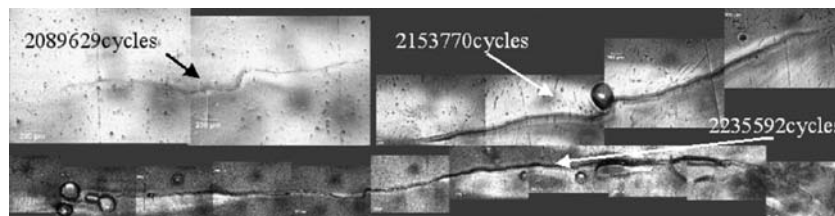


Figure 11. Replica images for HCF of 2024-T351 AL Alloy FSW polished mirror specimen at 270 MPa applied stress with load ratio $R = 0.1$

from the weakest regime which was identified to be located near the surface in the transition zone of the TMAZ and Flow Arm regimes.

4. Crack initiation was predominantly started at inclusion and porosity presence.

5. The Severely fractured surface in the triple point regime is due to trapped gaseous elements found located at 3mm depth from the surface.

6. Replica images depict the multiple cracking history and managed to capture the phenomenon of crack overlapping due to the different locations of the initiation sites.

7. The FSW process has not reached a state to provide a sound quality weld, and produces a subsurface crack from the defects that eliminate the Stage I crack propagation in fatigue.

Acknowledgement

The authors wish to thank Airbus UK Ltd for materials supplied, A. Ali was sponsored for this study through a Malaysian Ministry of Science (MOSTI) scholarship. Authors also wish to thank Malaysian Higher Education (MOHE) for a grant fundamental 02-01-07-035FR.

References

ASTM. (1988). Annual Book of ASTM Standards.

ASTM International, West Conshohocken, PA, USA.

Bussu, G. and Irving, P.E. (2001). Damage tolerance of welded aluminium aircraft structures. ICAF Design for Durability in the Digital Age. Proceedings of the 21st Symposium of the International Committee on Aeronautical Fatigue; June 27-29, 2001; Toulouse, France, p. 331-350.

Jata, K.V. and Semiatin, S.L. (2000). Continuous dynamic recrystallisation during friction stir welding of high aluminum alloys. Scripta Materialia, 43:743-749.

Kissell, J.R. and Malloy, B.J. (2001). Making aluminum more competitive in structural applications. In: Aluminium 2001- Proceedings of the TMS 2001 Aluminum Automotive and Joining Sessions. Das, S.K., Kaufman, J.G. and Lienert, T.J. (eds). TMS, Warrendale, PA, USA, p. 283-294.

Mendez, P.F. and Eagar, T.W. (2001). Welding processes for aeronautics. Adv. Mater. Process, 159(5):39-43.

Schmidt, H.J., Van, C., and Hanson, J. (2001). Tango metallic fuselage barrel validation of advanced technologies. ICAF Design for Durability in the Digital Age. Proceedings of the 21st Symposium of the International Committee on Aeronautical Fatigue; June 27-29, 2001; Toulouse, France, p. 273-288.